Improving motivation through real-time fMRI based self-regulation of the nucleus accumbens

Article · November 2017

DOI: 10.17863/CAM.14360

11 authors, including:

Li Su
University of Sheffield and University of Cambridge

Junchu Huang
South China University of Technology

Yi Wang
Chinese Academy of Sciences

Chao Yan
East China Normal University

American Psychological Association

Neuropsychology

0894-4105/18/$12.00

2018, Vol. 32, No. 6, 764–776
http://dx.doi.org/10.1037/neu0000425

Improving Motivation Through Real-Time fMRI-Based Self-Regulation of the Nucleus Accumbens

Zhi Li
Chinese Academy of Sciences, Beijing, China, and University of Chinese Academy of Sciences

Chen-yuan Zhang
Chinese Academy of Sciences, Beijing, China

Jia Huang and Yi Wang
Chinese Academy of Sciences, Beijing, China, and University of Chinese Academy of Sciences

Chao Yan
East China Normal University

Ke Li, Ya-wei Zeng, and Zhen Jin
Hospital 306, Beijing, China

Eric F. C. Cheung
Castle Peak Hospital, Hong Kong Special Administrative Region, China

Li Su
University of Cambridge

Raymond C. K. Chan
Chinese Academy of Sciences, Beijing, China, and University of Chinese Academy of Sciences

Objective: Impaired nucleus accumbens (NAcc) activation is associated with amotivation and anhedonia, which are resistant to treatment with antipsychotics and antidepressants in schizophrenia. In this study, healthy participants were trained to self-regulate the activation of their NAcc, a brain region that plays an important role in motivation, using real-time functional magnetic resonance imaging (fMRI) neurofeedback. ***Method:*** The experimental group ($N = 19$) received feedback from the NAcc, whereas the control group ($N = 5$) received "sham" feedback from the posterior parahippocampal gyrus, a control brain region not normally related to motivation. All participants were trained to use mental strategies to regulate their NAcc activations in a 3T MRI scanner. ***Results:*** For the learning effect of NAcc regulation, we found that the majority of participants (74%) in the experimental group successfully learned to self-regulate the NAcc. They also showed improved behavioral performance in motivation and decreased functional connectivity between the NAcc and the ventral medial prefrontal cortex and an increase in small-world properties in the reward circuit after training, indicating improved information integration in reward processing. However, improvement in motivation and modification of function connectivity were not observed in the *sham* control group and the participants who failed to self-regulate the NAcc in the

This article was published Online First July 26, 2018.

Zhi Li, Neuropsychology and Applied Cognitive Neuroscience Laboratory, CAS Key Laboratory of Mental Health, Institute of Psychology, Chinese Academy of Sciences, Beijing, China, and Department of Psychology, University of Chinese Academy of Sciences; Chen-yuan Zhang, Neuropsychology and Applied Cognitive Neuroscience Laboratory, CAS Key Laboratory of Mental Health, Institute of Psychology, Chinese Academy of Sciences; Jia Huang and Yi Wang, Neuropsychology and Applied Cognitive Neuroscience Laboratory, CAS Key Laboratory of Mental Health, Institute of Psychology, Chinese Academy of Sciences, and Department of Psychology, University of Chinese Academy of Sciences; Chao Yan, Key Laboratory of Brain Functional Genomics (MOE and STCSM), School of Psychology and Cognitive Science, East China Normal University; Ke Li, Ya-wei Zeng, and Zhen Jin, MRI Center, Hospital 306, Beijing, China; Eric F. C. Cheung, Castle Peak Hospital, Hong Kong Special Administrative Region, China; Li Su, Department of Psychiatry, University of Cambridge; Raymond C. K. Chan, Neuropsychology and Applied Cognitive Neuroscience Laboratory, CAS Key Laboratory of Mental Health, Institute of Psychology, Chinese Academy of Sciences, and Department of Psychology, University of Chinese Academy of Sciences.

This study was supported by National Natural Science Fund China Grants 91132701 and 81571317; Beijing Training Project for the Leading Talents in Science & Technology Grant Z151100000315020; Beijing Municipal Science & Technology Commission Grant Z161100000216138; "Strategic Priority Research Program (B)" of the Chinese Academy of Sciences Grant XDB02030002; the CAS Key Laboratory of Mental Health, Institute of Psychology, Chinese Academy of Sciences; and CAS/SAFEA International Partnership Programme for Creative Research Teams Grant Y2CX131003. Li Su's participation was funded by the NIHR Biomedical Research Centre and Biomedical Research Unit in Dementia, based at Cambridge University Hospitals NHS Foundation Trust and the University of Cambridge, and Alzheimer's Research UK.

Correspondence concerning this article should be addressed to Raymond C. K. Chan, Institute of Psychology, Chinese Academy of Sciences, Room 526, South Block, 16 Lincui Road, Beijing 100101, China, or to Li Su, China-United Kingdom Centre for Cognition and Ageing Research, Faculty of Psychology, Southwest University, 2 Tiansheng Road, Chongqing, China. E-mail: rckchan@psych.ac.cn or ls514@cam.ac.uk

experimental group. Self-regulation was influenced by the baseline motivation. ***Conclusions:*** These findings suggest that the NAcc could be self-regulated using real-time fMRI neurofeedback and can result in improved motivation in cognitive tasks.

General Scientific Summary
This study applied real-time functional magnetic resonance imaging (fMRI)-based neurofeedback to volitionally regulate the nucleus accumbens (NAcc). Our findings demonstrated that the NAcc activation could be self-regulated. Of importance, people who successfully learned to self-regulate NAcc activation showed significant improvement in motivation and functional connectivity in the reward circuit. This study demonstrated the potential efficacy of a nonpharmaceutical intervention in alleviating resistant negative symptoms of schizophrenia using real-time fMRI neurofeedback.

Keywords: real-time fMRI, nucleus accumbens, motivation, generalization effect, reward

Supplemental materials: http://dx.doi.org/10.1037/neu0000425.supp

The nucleus accumbens (NAcc) has been widely considered as a brain center underlying motivation and reward (Berridge, 2007; Berridge & Robinson, 1998). The dopaminergic system including the NAcc is associated with incentive salience that attributes value to various rewards and facilitates goal-directed behaviors (Berridge & Robinson, 1998; Wyvell & Berridge, 2000). Other hypothesis and relevant evidence have also linked the NAcc with hedonic experience (Berridge, 2003; Kringelbach & Berridge, 2009; Wacker, Dillon, & Pizzagalli, 2009), effort-related processes (Salamone, Correa, Farrar, Nunes, & Pardo, 2009), and reward prediction (Schultz, 1998; Schultz, Dayan, & Montague, 1997), which jointly constitute various aspects of motivation and pleasure. Empirical evidence has suggested that dysfunction of the NAcc or the ventral striatum in patients with schizophrenia (Juckel, Schlagenhauf, Koslowski, Filonov, et al., 2006; Juckel, Schlagenhauf, Koslowski, Wüstenberg, et al., 2006; Radua et al., 2015), major depression (Knutson, Bhanji, Cooney, Atlas, & Gotlib, 2008; Pizzagalli et al., 2009), and addiction (Beck et al., 2009; Wrase et al., 2007) are associated with negative symptoms, amotivation, and anhedonia (Kring & Barch, 2014; Pizzagalli, 2014), which are resistant to treatment with antipsychotics and antidepressants (Kring & Barch, 2014; Pizzagalli, 2014).

Advances in neuroimaging have provided opportunities for alternative nonpharmaceutical interventions to alleviate amotivation and anhedonia. Real-time functional magnetic resonance imaging (rtfMRI) neurofeedback, which is noninvasive and has millimeter spatial resolution (deCharms, 2008; Sulzer, Haller, et al., 2013), has been successfully applied to self-regulate the activation of the anterior cingulate cortex (Cordes et al., 2015; Mathiak et al., 2015), the amygdala (Paret et al., 2014; Zotev et al., 2011), the dorsal lateral prefrontal cortex (Sherwood, Kane, Weisend, & Parker, 2016; Zhang, Yao, Zhang, Long, & Zhao, 2013), the insula (Lawrence et al., 2014; Sitaram et al., 2014) and the mesolimbic system (Greer, Trujillo, Glover, & Knutson, 2014; Sulzer, Sitaram, et al., 2013). Greer and colleagues (2014) found that NAcc activation could be self-regulated through rtfMRI-based neurofeedback. However, due to differences in methodology and the lack of understanding of its underlying neurobiology, it is not clear whether rtfMRI training could lead to clinically meaningful behavioral changes. To develop this technique further and investigate its clinical utility, it is important to understand the neurobiological mechanisms behind self-regulation based on computationally defined learning theories as well as other factors that influence the effectiveness of rtfMRI neurofeedback (Lawrence et al., 2014). This study aimed to examine individual differences during neurofeedback and further explored the neurobiological mechanism and generalization effect of real-time fMRI neurofeedback training of the NAcc.

As a hub of pleasure experience and reward processing (Berridge, 2007; Kringelbach & Berridge, 2009), the NAcc is engaged in various aspects of motivation. In this study, we employed several cognitive tasks to validate the generalization effect of rtfMRI-based neurofeedback training of NAcc activation, including whether neurofeedback can improve the various aspects of motivation and the reward circuit. Moreover, the functional connectivity between the NAcc and the ventral medial prefrontal cortex (vmPFC) is implicated in reward processing and pleasure experience (Cauda et al., 2011; Ferenczi et al., 2016; Greer et al., 2014; Schlaepfer et al., 2008; Wacker et al., 2009). Volitional regulation of the NAcc has been shown to alter the functional connectivity between the NAcc and the vmPFC during tasks (Greer et al., 2014). However, no study has investigated the task-independent functional connectivity changes. Hence we also explored whether the resting-state functional connectivity between the NAcc and the vmPFC could be regulated by rtfMRI-based neurofeedback training. The ability to regulate task-free properties of the reward circuit is important for the generalization effect and clinical applications.

The third focus of this study was to find a way to classify individuals into those who are suitable for learning to control their NAcc activation. Although many studies have demonstrated the effectiveness of rtfMRI-based neurofeedback training at the group level, the effectiveness of volitional regulation of target brain areas may be different for different individuals (Sulzer, Haller, et al., 2013). Similar to other pharmacological and nonpharmacological interventions, rtfMRI neurofeedback is unlikely to be a "one size fits all" intervention. Identifying the possible factors that influence the effectiveness of NAcc self-regulation may pave the way for clinical application and personalized intervention.

We hypothesized that NAcc activation could be self-regulated using rtfMRI neurofeedback. We also hypothesized that not all the participants could learn to regulate their NAcc activation and that the effectiveness is related to neuropsychological factors of each participant. Last, we hypothesized that participants who were able to self-regulate their NAcc activation equally well between the NAcc and the vmPFC would show improved motivation and modified functional connectivity.

Method

Participants

Twenty-five healthy female postgraduates were recruited from the University of the Chinese Academy of Sciences in this study. Exclusion criteria included (a) personal or family history of diagnosable mental disorders, (b) a history of head trauma or encephalopathy, (c) a history of substance abuse, and (d) menstruation in the past 2 weeks. The screening of a personal or family history of mental disorders was confirmed by a semistructured interview and self-reports. All participants were randomly divided into two groups: the experimental group ($N = 20$) receiving actual feedback from the NAcc, and the *sham* control group ($N = 5$) receiving sham feedback from the posterior parahippocampal gyrus. One participant in the experimental group did not complete the imaging protocol and was subsequently excluded from the study. The Ethics Committees of the corresponding institutions involved in this project approved the study. Informed consent was obtained from all participants.

Procedure

For each participant in both the experimental and control groups, the whole experiment was conducted in 4 consecutive days. On the first day, participants were required to complete several questionnaires, including the Temporal Experience Pleasure Scale (TEPS; Chan et al., 2012; Gard, Gard, Kring, & John, 2006), the Behavioral Inhibition System/Behavioral Activation System scale (BIS/BAS; Carver & White, 1994; Li et al., 2008), the effort expenditure for rewards task (EEfRT; Treadway, Buckholtz, Schwartzman, Lambert, & Zald, 2009), and the anticipatory and consummatory pleasure task (ACP; Heerey & Gold, 2007; Lui et al., 2016). The abbreviated Chinese version of the Wechsler Adult Intelligence Scale was used to estimate the IQ of the participants (Gong, 1992). In the morning of the second day, a high-resolution structural MRI brain scan and a 6-min resting-state image were acquired from each participant. In addition, participants were asked to complete three runs of the functional monetary incentive delay (MID) task in the scanner (pretest session). In the afternoon of the second day and the morning of the third day, participants received two five-run sessions of rtfMRI-based neurofeedback training (training Session 1 and Session 2). In the afternoon of the third day, a 6-min resting-state image and three runs of functional MID were acquired from each participant (posttest session). Finally, on the fourth day, all participants completed the same questionnaires and behavioral paradigms as on the first day (see Figure 1A). Please refer to the online supplemental materials for details of each questionnaire and the behavioral and functional imaging paradigms.

Real-Time fMRI ROI Selection

Before the training Session 1 and after the pretest session, the target region of interest (ROI) of the bilateral NAcc (size = 65 3 mm × 3 mm × 3 mm voxels), the *sham* control target ROI at the bilateral posterior parahippocampal gyrus (size = 746 3 mm × 3 mm × 3 mm voxels), and the reference ROI at the bilateral lingual cortex (size = 2,135 3 mm × 3 mm × 3 mm voxels) were defined based on the brain structural T1 image of each participant. This was done by inverse-coregistering the predefined ROIs from the Harvard-Oxford atlas with SPM 8 (Friston, 2007) to ensure that the ROI selection was consistent among all participants. The reference ROI was used to control for global brain effect.

Real-Time fMRI Mental Strategies

Each run of both training sessions consisted of five 30-s baseline blocks interleaved with five 30-s regulation blocks, which were administered alternately with a 15-s interval between each block. During the regulation block, participants were asked to turn the pointer on a semicircle dashboard to the right (increase), using provided mental strategy “to expect the forthcoming positive events in the future three months.” This mental strategy has been applied successfully to regulate NAcc activations in a previous study (Greer et al., 2014). Participants were also informed that the visual display of the feedback had a delay of 4–5 s that was mainly caused by the natural delay of hemodynamic function.

During the baseline block, participants were required to turn the pointer to the left on the feedback screen (decrease). The mental strategy “to do mental arithmetic such as to minus 3 from 100” was provided in the baseline blocks. The mental calculation was a general strategy used during the baseline−decrease phase in previous studies (Sulzer, Haller, et al., 2013; Lawrence et al., 2014; see Figure 1 B).

Functional Imaging Paradigm

The functional MID task has been found to be sensitive in detecting NAcc activation in humans in vivo (Knutson, Fong, Adams, Varner, & Hommer, 2001; Knutson, Westdorp, Kaiser, & Hommer, 2000). In each trial of the MID task, a cue indicated monetary gain, loss, or neutral condition was first presented, followed by a blue target that was required to be hit. The duration of each trial was 12 s. Participants obtained monetary points if the target was hit in the monetary gain condition and lost monetary points if the target was missed in the monetary loss condition. Each scan contained three runs of that task, and each run contained nine trials of each condition presented pseudorandomly (please see our previous study, Chan et al., 2016, for details).

Image Data Acquisition

All participants underwent MRI scans in a Siemens 3T scanner with a 32-channel head coil using a $T2^*$ echo planar imaging sequence (TR = 2,000 ms; TE = 30 ms; FOV = 210 mm; slices = 32; flip angle = 90 degrees; image matrix = 64 × 64; voxel dimensions = 3.3 mm × 3.3 mm × 4 mm) for resting-state, task-based functional MRI and real-time neurofeedback training as well as a high resolution T1 structural brain image (TR = 2,300 ms; TE = 3 ms; FOV = 256 mm; flip angle = 9 degrees; image matrix = 256 × 256; voxel dimensions = 1 mm × 1 mm × 1 mm). Head movement was reduced with a head-holder pad placed between the head coil and the participants’ heads.

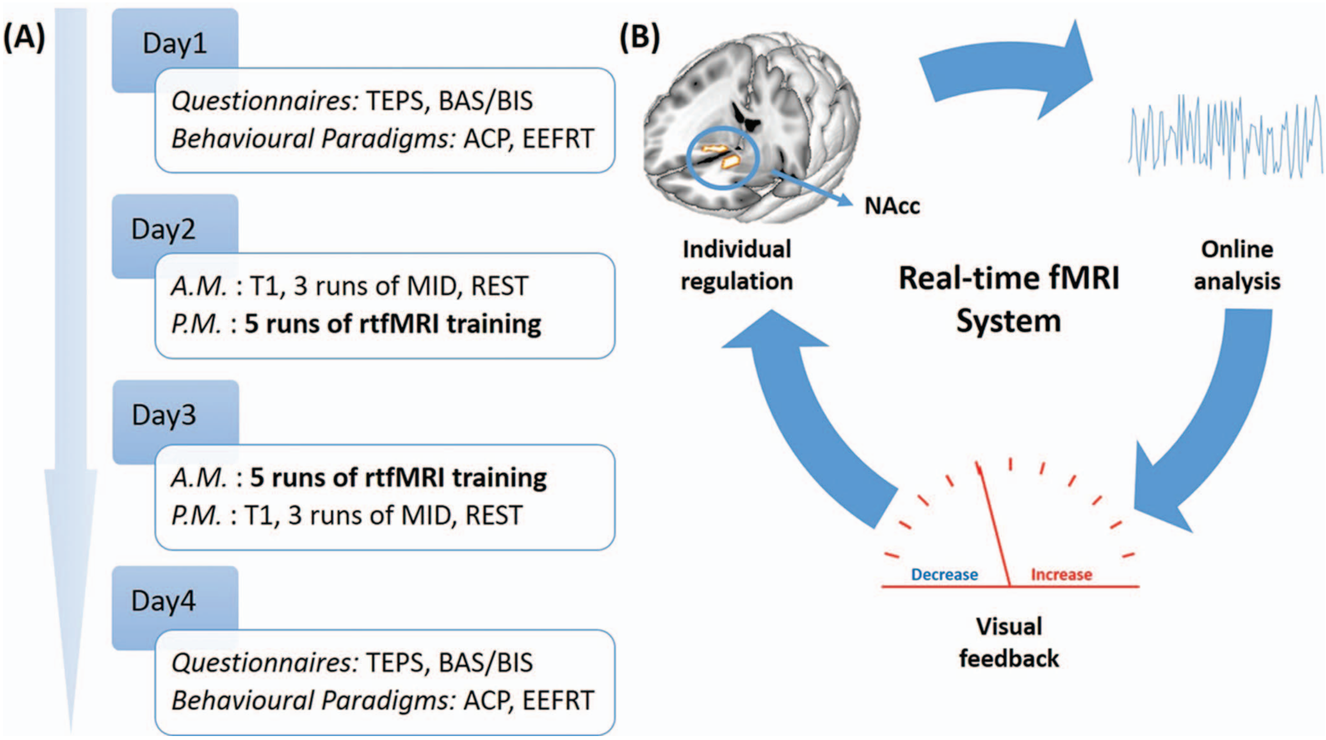

Figure 1. Experimental procedure. Panel A: The experimental procedure and real-time functional magnetic resonance imaging neurofeedback training system for the whole experiment. TEPS = Temporal Experience Pleasure Scale; BAS = Behavioral Activation System; BIS = Behavioral Inhibition System; ACP = anticipatory and consummatory pleasure task; EEFRT = effort expenditure for rewards task; T1 = structural image; MID = monetary incentive delay task; REST = resting-state functional image; rtfMRI = real-time functional magnetic resonance imaging. Panel B: The real-time activation of the nucleus accumbens (NAcc) was drawn out and processed online, and then the calculated value was presented on a dashboard. Participants were required to control the pointer on the dashboard through the difference strategies during the baseline and training blocks. See the online article for the color version of this figure.

Real-Time fMRI Online Analysis and Neurofeedback

Real-time fMRI data analysis was carried out using a customized pipeline combining SPM, fieldtrip, and in-house MATLAB (The MathWorks, Inc., Natick, Massachusetts, United States) scripts as well as the built-in real-time image reconstruction system of the Siemens scanner. Each volume acquired from the scanner was transferred to another workstation computer via network immediately after image reconstruction and then preprocessed with temporal and spatial corrections. The blood oxygen level-dependent (BOLD) signal from the target ROI in the experimental group (or sham ROI in the control group) and reference ROI were extracted in real time. The visual feedback, that is, the position of the pointer, on the visually displayed dashboard during the training was calculated with the following formula: Feedback = ROI_{target} ($BOLD_{regulation}$ − $\overline{BOLD}_{baseline}$) − $ROI_{reference}$ ($BOLD_{regulation}$ − $\overline{BOLD}_{baseline}$), where $BOLD_{regulation}$ refers to the BOLD signal from the corresponding ROI of each volume, whereas $\overline{BOLD}_{baseline}$ refers to the average BOLD signal from the corresponding ROI of the preceding baseline block. The visual feedback was displayed to the participant in the scanner. To minimize fluctuation due to noise from the BOLD signal, we smoothed the feedback signal using a three-point temporal average with weightings set at .125, .25, and .625 for the current and two preceding blocks (Lawrence et al., 2014). As previously explained, the target ROI of the experimental group was the NAcc, whereas the target ROI of the *sham* control group was the posterior parahippocampal gyrus. The reference ROI at the lingual cortex and the *sham* control target ROI were chosen because these areas were normally not engaged in reward processing. They were used to control for nonspecific BOLD changes due to other factors, such as respiration (Lawrence et al., 2014).

Offline Image Data Analysis

All the functional images including the rtfMRI-based neurofeedback training data, the functional MID tasks, and the resting-state data were temporally and spatially corrected for slice timing and motion artifacts. They were then nonlinearly normalized to the Montreal Neurological Institute (MNI) space. The Friston-24 parameter model regression was adopted to address the head movement measured by the three-transition and three-rotation parameters (Friston, Williams, Howard, Frackowiak, & Turner, 1996; Yan, Craddock, He, & Milham, 2013). All the images were resampled into $3 \times 3 \times 3$ mm^3 resolution. The rtfMRI-based neurofeedback training data and the functional MID data were smoothed with a Gaussian kernel of 8 mm full width at half maximum (FWHM), whereas the resting-state data were smoothed with a Gaussian kernel of 4 mm FWHM and detrended to control for slow frequency scanner shift. Data preprocessing of resting state fMRI was carried out using the Dpabi toolbox (Yan, Wang, Zuo, & Zang, 2016), which integrates functions from SPM, AFNI (Cox, 1996), and FSL (Jenkinson, Beckmann, Behrens, Woolrich, & Smith, 2012).

We then extracted the BOLD signal from both the baseline and regulation blocks from each voxel of the NAcc. The head-movement parameters were regressed from the extracted signals. For each individual datum, the residuals obtained from the aforementioned step were averaged among each block from which a 10 (block) $\times$ 65 (voxel of the NAcc) matrix was acquired. The conventional whole brain−based generalized linear model was not adopted in this study because the BOLD signal was the feedback we presented; hence, the increasing raw BOLD signal was meaningfully interpreted. To classify the participants into the learning and nonlearning groups within each of the two training sessions, we inputted the differences between the mean of every regulation block and its preceding baseline block (representing the regulation effect for each block) into a general linear model and tested whether the regulation effect increased over time. If the beta value was significantly ($p < .05$) larger than zero, which indicated that the differences were increasing over time with the training runs, we regarded that the participant had successfully learned to control NAcc activation. Otherwise, if NAcc activation did not change over time during the neurofeedback, we classified the participant as a nonlearner. Based on this criterion, we divided the participants in the experimental group into two subgroups: (a) the *learning group,* which successfully learned to control NAcc activation in either or both of the two training sessions, and (b) the *nonlearning group,* which did not learn to control NAcc in both training sessions (see Tables 1 and 2 in the online supplemental materials for more details of this analysis).

Image Analysis of the MID Task and Resting-State fMRI Data

Three anticipatory cues that corresponded to monetary gain, monetary loss, and monetary neutral; six consummatory outcomes that contained monetary gain hit, monetary gain miss, monetary loss hit, monetary loss miss, monetary neutral hit, and monetary neutral miss; and the target hit period of the MID task were modeled into a general linear model. The three parameters of rotation and three parameters of transition were also included in the general linear model as the covariates to control for the head motion. The percentage of signal changes of the monetary gain and monetary loss conditions was then drawn out from the NAcc for group analysis. To confirm the activation of NAcc during the anticipation of monetary gain and loss, we conducted small volume correction of the NAcc on the contrasts between (a) monetary gain greater than monetary neutral and (b) monetary loss greater than monetary neutral (see Table 3 in the online supplemental materials). The threshold was set to $p < .05$ with family-wise error correction. The reaction time (RT) during the target hit period for the three different anticipatory conditions was also calculated as the behavioral measure of motivation.

Functional connectivity defined by the z-transformation of the correlation coefficient between the NAcc and the vmPFC was calculated based on the resting-state fMRI image. We also constructed an a priori reward circuit based on previous studies (Haber & Knutson, 2010; Kringelbach & Berridge, 2009; Pizzagalli, 2014) with connectivity comprising a total of 28 regions (the bilateral substantia nigra, the bilateral NAcc, the bilateral putamen, the bilateral caudate, the bilateral thalamus, the bilateral amygdala, the bilateral insula, the bilateral lateral globus pallidus, the bilateral medial globus pallidus, the bilateral DLPFC, the bilateral vmPFC, bilateral inferior OFC, the bilateral middle OFC, and the bilateral superior OFC). The regions of interest (ROIs) adopted in this study were obtained from the Automated Anatomical Labeling atlas (Tzourio-Mazoyer et al., 2002). In the data set for each participant, a correlation matrix was constructed from the time series correlation of each ROI. In network theory (Watts & Strogatz, 1998), C_p denotes the average clustering coefficients across all the nodes, whereas L_p denotes the average shortest path length between each pair of nodes. The C_p and L_p of the reward circuit were compared with 100 random networks. A small world would be featured with the following conditions: $\gamma = C_p^{real}/C_p^{rand} > 1$, $\lambda = L_p^{real}/L_p^{rand} \sim 1$, and $\sigma = \gamma/\lambda > 1$. The small-world properties of the reward circuit were calculated based on sparsity ranging from .1 to .4 with a .01-step length in the GRETNA toolbox (Wang et al., 2015). We did not perform global signal regression on the resting-state functional image, due to the ongoing debate on its reliability (Murphy, Birn, Handwerker, Jones, & Bandettini, 2009; Saad et al., 2012).

Statistical Tests

Using SPSS 18, we first compared the demographics, baseline motivation, and functional connectivity of the experimental group with the *sham* control using the Mann–Whitney U test. Then the changes observed in the behavioral tests before and after rtfMRI training were compared using the Wilcoxon signed-ranks test in both the experimental and the *sham* control groups. These tests included self-reported questionnaires, behavioral performances (e.g., RT and NAcc activation in the MID task), functional connectivity between the NAcc and the vmPFC, and small-world properties of the reward circuit. Finally, the same nonparametric tests were used to compare the learning and the nonlearning groups in terms of the corresponding changes before and after the neurofeedback training.

Results

Training Effect

Nine participants in training Session 1 and 10 participants in training Session 2 in the experimental group successfully learned to self-regulate their NAcc activation (see Figure 2). Over 14 participants (73.68%) in the experimental group successfully learned to self-regulate their NAcc activation in at least one training session. The remaining five participants from the experimental group who failed to regulate NAcc activation in both sessions were classified into the nonlearning group. The training effect of each participant is reported in Table 1 in the online supplemental materials. In the *sham* control group, three partici-

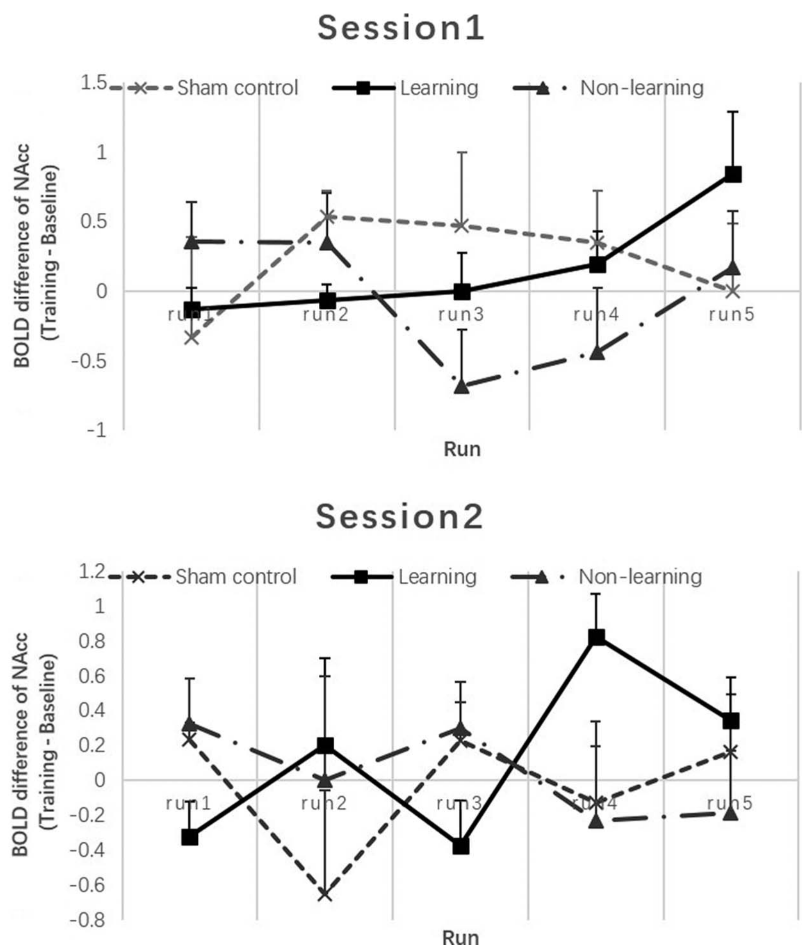

Figure 2. Training effect. The real-time functional magnetic resonance imaging training on the self-regulation of nucleus accumbens (NAcc) activation. The *x*-axis denotes the runs, and the *y*-axis denotes the blood oxygen level-dependent (BOLD) difference in NAcc between the training block with the previous baseline block. Error bars indicate error of the means.

pants in training Session 1 and one participant in training Session 2 successfully learned to regulate posterior parahippocampal activation. Only one participant learned to self-regulate the NAcc activation in both Session 1 and Session 2 (see Tables 1 and 2 in the online supplemental materials).

Generalization Effect

There was no significant difference between the experimental group and the *sham* control group in baseline demographics and motivation behavioral performance. At baseline, we found no significant group difference in functional connectivity between the NAcc and the vmPFC, except that the experimental group showed significantly lower press rates to avoid undesirable pictures in the ACP task (see Table 1). In the experimental group, the press rate to seek desirable pictures (p = .009, Cohen's d = −.43) and to avoid undesirable pictures (p = .003, Cohen's d = −.85) were both increased after the rtfMRI-based neurofeedback training. Furthermore, their RT to hit the target in the MID task was decreased during the anticipation of monetary gain (p = .002, Cohen's d = .79) and monetary loss (p = .003, Cohen's d = .77). The experimental group showed significantly decreased functional connectivity between the left NAcc and the left vmPFC (p = .011, Cohen's d = .89) and the right vmPFC (p = .033, Cohen's d = .73) and between the right NAcc and the right vmPFC (p = .033, Cohen's d = .72; see Table 1). However, no improvement in performance in behavioral tasks and no change in functional connectivity were observed in the *sham* control group. Both the experimental and *sham* control groups failed to show significant changes on the EEfRT task and small-world properties of the reward circuit before and after training (see Table 1 and Figure 3).

Individual Differences in Neurofeedback

To explore which personality and neurophysiological trait predicted the effectiveness of neurofeedback training, we compared the baseline variables of the nonlearning group (N = 5) with those of the learning group (N = 14). The two groups were not significantly different in demographics (see Table 2). We found that the learning group showed a significantly higher Drive score on the BAS (p = .028, Cohen's d = −1.43). Participants in the learning group were more likely to choose a hard task in the middle (p =

Table 1
Generalization Effect of Volitional Regulation on the NAcc in the Experimental and Sham Control Groups

Variable	*Sham* control group ($N = 5$)				Experimental group ($N = 19$)				Baseline group difference	
	Before	After	p	Cohen's d	Before	After	p	Cohen's d	p	Cohen's d
Age	24.2 (.84)				25.84 (2.39)				.122	−.92
IQ	123.6 (6.66)				121.16 (7.65)				.352	.34
Education (years)	17.6 (1.14)				18.63 (1.77)				.129	−.69
TEPS_TOT	96.8 (7.4)				89.16 (13.21)				.176	.71
TEPS_ANT	41.6 (4.56)				40.16 (7.27)				.722	.24
TEPS_CON	53.4 (4.34)				46.05 (8.18)				.064	1.12
BAS_Drive	6.2 (1.3)				7.21 (2.2)				.369	−.56
BAS_Fun_Seeking	6.8 (1.48)				6.95 (2.07)				.943	−.08
BAS_Reward	7.8 (2.39)				7.84 (2.63)				.884	−.02
BIS	9.8 (4.32)				10.21 (2.49)				.35	−.12
ACP (presses per second)										
Negative slides	7.51 (1.51)	7.53 (1.56)	.345	−.01	5.56 (1.82)	6.35 (1.93)	.003**	−.43	.012*	1.23
Positive slides	6.79 (2.61)	7.47 (.97)	.893	−.35	4.8 (2.45)	6.63 (1.79)	.009**	−.85	.095	.8
EEfRT (%)										
Low (12%)	.64 (.35)	.6 (.38)	1	.11	.69 (.29)	.75 (.36)	.507	−.18	.855	−.15
Middle (50%)	.97 (.07)	1 (0)	.317	−.63	.96 (.09)	.99 (.04)	.157	−.49	.92	.12
High (88%)	1 (0)	1 (0)	1		.98 (.06)	1 (0)	.18	−.47	.459	.47
MID										
RT_Loss	216.9 (11.56)	207.83 (13)	.138	.74	230.65 (17.45)	218.33 (14.48)	.003**	.77	.11	−.93
RT_Gain	219.93 (16.87)	203.76 (15.8)	.08	.99	227.51 (17.3)	213.91 (17.18)	.002**	.79	.414	−.44
NAcc_Loss	−.22 (.39)	.21 (.39)	.08	−1.09	−.13 (.63)	.18 (.64)	.107	−.49	.804	−.16
NAcc_Gain	−.05 (.19)	.24 (.43)	.225	−.86	−.03 (.6)	.25 (.7)	.227	−.42	.859	−.05
Functional connectivity										
L_NAcc-L_vmPFC	.48 (.08)	.27 (.25)	.138	1.1	.42 (.11)	.3 (.17)	.011*	.89	.499	.54
L_NAcc-R_vmPFC	.46 (.11)	.27 (.19)	.138	1.23	.42 (.12)	.3 (.18)	.033*	.73	.644	.39
R_NAcc-L_vmPFC	.44 (.14)	.25 (.17)	.138	1.17	.37 (.14)	.29 (.22)	.136	.45	.337	.47
R_NAcc-R_vmPFC	.45 (.16)	.29 (.13)	.225	1.13	.41 (.15)	.27 (.24)	.033*	.72	.644	.28

Note. Data represent means, with standard errors in parentheses. NAcc = nucleus accumbens; IQ = intelligence quotient; TEPS = total score on the Temporal Experience Pleasure Scale; TOT = Total score; ANT = Anticipatory subscale; CON = Consummatory subscale; BAS = Behavioral Activation System; BIS = Behavioral Inhibition System; ACP = anticipatory and consummatory pleasure task; EEfRT = effort expenditure of reward task; MID = monetary incentive delay task; RT = reaction time; L = left; R = right; vmPFC = ventral medial prefrontal cortex.
* $p < .05$. ** $p < .01$.

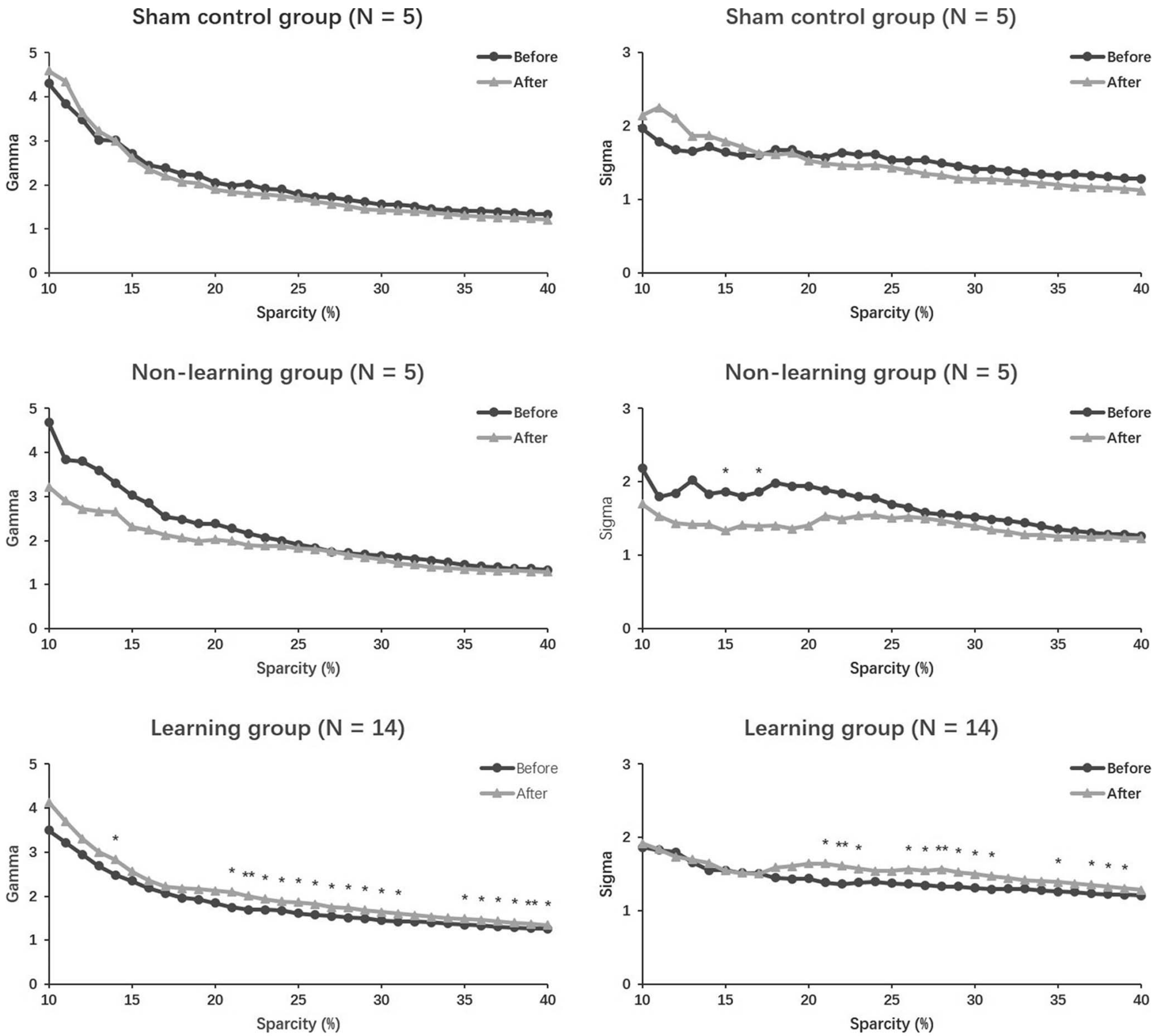

Figure 3. Group difference on the topological properties of brain functional connectivity. The difference before and after the real-time functional magnetic resonance imaging (fMRI) training on the small-world properties γ and σ of the reward circuit. The *x*-axis denotes the difference in sparsity of the network, whereas the *y*-axis denotes the values of γ or σ. The learning group showed improved small-world properties γ and σ of the reward circuit after the real-time fMRI self-regulation on the nucleus accumbens activation that was absent in the nonlearning and *sham* control groups.

.013, Cohen's $d = -1.17$) and high ($p = .015$, Cohen's $d = -1.03$) reward disparity of the EEfRT task compared with the nonlearning group. In addition, the learning group also showed a trend in having higher NAcc activation during the anticipation of monetary gain in the MID task ($p = .052$, Cohen's $d = -1.18$; see Table 2).

Compared with the nonlearning group, the learning group showed an increased press rate to seek desirable pictures ($p = .005$, Cohen's $d = -.96$) and to avoid undesirable pictures ($p = .002$, Cohen's $d = -.58$) in the ACP task and reduced RT to hit the target in the MID task during the anticipation of monetary gain ($p = .019$, Cohen's $d = .89$) and monetary loss ($p = .005$, Cohen's $d = 1.1$) after rtfMRI-based neurofeedback training. Moreover, the learning group showed significantly decreased functional connectivity between the left NAcc and the left vmPFC ($p = .013$, Cohen's $d = 1.12$) and the right vmPFC ($p = .035$, Cohen's $d = .89$), and there was a decrease in functional connectivity between the right NAcc and the right vmPFC with trend significance ($p = .064$, Cohen's $d = .73$; see Table 2). The small-world properties of the reward circuit in the learning

Table 2
Generalization Effect of Volitional Regulation on the NAcc of the Learning and Nonlearning Groups

Variable	Nonlearning group (N = 5)				Learning (N = 14)				Baseline group difference	
	Before	After	p	Cohen's d	Before	After	p	Cohen's d	p	Cohen's d
Age	27.4 (1.82)				25.29 (2.37)				.085	1
IQ	120.4 (11.74)				121.43 (6.2)				.815	−.11
Education (years)	19.8 (1.48)				18.21 (1.72)				.073	.99
TEPS_TOT	95.4 (14.89)				86.93 (12.38)				.211	.62
TEPS_ANT	39.8 (7.63)				40.29 (7.44)				.189	−.06
TEPS_CON	51.4 (7.57)				44.14 (7.75)				.487	.95
BAS_Drive	5.4 (1.14)				7.86 (2.14)				.028*	−1.43
BAS_Fun_Seeking	6.4 (1.67)				7.14 (2.21)				.512	−.38
BAS_Reward	6.8 (.84)				8.21 (2.97)				.412	−.65
BIS	11.4 (1.52)				9.79 (2.67)				.322	.74
ACP (presses per second)										
Negative slides	5.15 (1.09)	5.04 (1.3)	.893	.09	5.71 (2.05)	6.86 (1.92)	.002**	−.58	.643	−.19
Positive slides	5.24 (2.07)	6.13 (1.82)	.5	−.46	4.63 (2.65)	6.82 (1.82)	.005**	−.96	.579	.26
EEfRT (%)										
Low (12%)	.57 (.22)	.47 (.43)	.686	.27	.73 (.3)	.85 (.29)	.106	−.38	.117	−.62
Middle (50%)	.87 (.14)	.97 (.07)	.257	−.89	.99 (.04)	1 (0)	.317	−.38	.013*	−1.17
High (88%)	.93 (.1)	1 (0)	.18	−1.03	1 (0)	1 (0)	1.000	—	.015*	−1.03
MID										
RT_Loss	233.05 (27.24)	225.44 (20.67)	.225	.31	229.79 (13.79)	215.79 (11.5)	.005**	1.10	.643	.15
RT_Gain	235.57 (23.19)	220.29 (24.16)	.043*	.65	224.64 (14.67)	211.63 (14.42)	.019*	.89	.308	.56
NAcc_Loss	−.52 (.75)	−.04 (.61)	.225	−.70	.01 (.55)	.25 (.65)	.245	−.41	.165	−.79
NAcc_Gain	−.52 (.61)	−.06 (.73)	.225	−.67	.15 (.52)	.36 (.68)	.551	−.35	.052†	−1.18
Functional connectivity										
L_NAcc-L_vmPFC	.39 (.12)	.34 (.2)	.686	.31	.44 (.11)	.28 (.16)	.013*	1.12	.579	−.35
L_NAcc-R_vmPFC	.44 (.12)	.39 (.18)	.686	.30	.41 (.12)	.27 (.17)	.035*	.89	.459	.29
R_NAcc-L_vmPFC	.42 (.09)	.33 (.17)	.5	.65	.36 (.15)	.28 (.23)	.272	.41	.643	.53
R_NAcc-R_vmPFC	.5 (.11)	.36 (.24)	.345	.70	.38 (.15)	.24 (.23)	.064†	.73	.195	.87

Note. Data represent means, with standard errors in parentheses. NAcc = nucleus accumbens; IQ = intelligence quotient; TEPS = total score on the Temporal Experience Pleasure Scale; TOT = Total score; ANT = Anticipatory subscale; CON = Consummatory subscale; BAS = Behavioral Activation System; BIS = Behavioral Inhibition System; ACP = anticipatory and consummatory pleasure task; EEfRT = effort expenditure of reward task; MID = monetary incentive delay task; RT = reaction time; L = left; R = right; vmPFC = ventral medial prefrontal cortex.
† Trend is significant. * $p < .05$. ** $p < .01$.

group were also increased with sparsity ranging from .21 to .4 after the whole training (see Figure 3). Changes in behavioral performance, functional connectivity, and small-world properties of the reward circuit were not observed in the nonlearning group (see Table 2 and Figure 3).

Discussion

In this study, we found that activity of the NAcc could be self-regulated through rtfMRI-based neurofeedback training. Increased motivation measured by behavioral and functional imaging paradigms, as well as decreased functional connectivity between the NAcc and the vmPFC, were observed in the experimental group but not in the *sham* control group, after two sessions of training on self-regulation of the NAcc. As expected, not all participants were capable of learning to control NAcc activation after two training sessions in our study. Participants who successfully learned to regulate their NAcc had higher trait motivation than did nonlearning participants.

Self-regulation of the NAcc was achieved by the rtfMRI-based neurofeedback training in this study, which corroborated previous findings (Greer et al., 2014; Kirsch, Gruber, Ruf, Kiefer, & Kirsch, 2016; MacInnes, Dickerson, Chen, & Adcock, 2016), suggesting that rtfMRI feedback technology could mediate the activation of not only superficial cortical areas (Sherwood et al., 2016; Zhang et al., 2013) but also deep subcortical structures in the mesolimbic system (Greer et al., 2014; Sulzer, Sitaram, et al., 2013). Empirical evidence has suggested that NAcc activation is associated with the anticipation of rewarding stimuli (Knutson et al., 2000, 2001; Knutson & Gibbs, 2007). It has been argued that the ability to anticipate future rewards such as positive events can activate the NAcc; thus, increasing the activity in the NAcc using neurofeedback training (Greer et al., 2014) may improve anhedonia (Favrod, Giuliani, Ernst, & Bonsack, 2010; Nguyen et al., 2016). The multiple-session training strategy adopted in this study is different from that used in previous similar studies on rtfMRI-based neurofeedback training on the NAcc (Greer et al., 2014; Kirsch et al., 2016; MacInnes et al., 2016). The longer length of training could increase the likelihood of acquiring NAcc self-regulation in our participants.

Most important, we found a generalization effect of the rtfMRI-based neurofeedback training that was less robust. After two rtfMRI-based neurofeedback training sessions, the learning group showed an accelerated response to acquire desirable affective pictures or to avoid undesirable affective pictures during the anticipatory phase of the ACP task and faster RT during the anticipation of monetary gain or loss in the MID task. Taken together, our results provide empirical evidence supporting the potential use of rtfMRI-based neurofeedback training in the intervention of refractory negative symptoms such as amotivation and anhedonia.

Participants in the experimental group, who successfully learned to regulate the NAcc, showed weakened functional connectivity between the NAcc and the vmPFC, both of which are engaged in reward processing and pleasure experience (Cauda et al., 2011; Wacker et al., 2009). Consistent with our findings, Schlaepfer et al. (2008) found a significant decrease in activation in the vmPFC after deep brain stimulation at the NAcc in patients with major depression. In addition, Ferenczi et al. (2016) used optogenetic fMRI to manipulate the brainwide neural activity of rats and found that increases in mPFC activity reduced dopaminergic activity in the NAcc and relevant behavioral drive for dopaminergic stimulation. This suggests that inhibitory projections from the vmPFC to the NAcc can be altered by regulating NAcc activity in both humans and animals, and this neural mechanism may underlie our findings of reduced functional connectivity between the vmPFC and the NAcc. In a previous resting-state fMRI study, patients with first-episode schizophrenia exhibited hyperconnectivity between the vmPFC and the NAcc (Fornito et al., 2013). The rtfMRI-based neurofeedback training on NAcc activation may provide a potential noninvasive intervention to normalize this hyperconnectivity in schizophrenia. However, one should interpret these findings cautiously due to the relatively small sample size in the *sham* control group. Although the pre- and posttraining comparisons on functional connectivity in the *sham* control group were not significant, the effect sizes were close to what we found in the experimental group. Future studies recruiting a larger sample size of *sham* control should be conducted to replicate and extend our findings.

We also observed improvements in the network properties of the reward circuitry after rtfMRI-based neurofeedback training in the learning group. The increased small-world property γ and σ of the reward circuity in the learning group suggests that the reward circuit had become more efficient in information processing after the training. The disrupted reward network and the ventral striatal dopaminergic system play a vital role in amotivation and anhedonia in schizophrenia and major depression (Kring & Barch, 2014; Pizzagalli, 2014; Radua et al., 2015). Improving the small-world properties of the reward circuit in these patients using rtfMRI neurofeedback may have potential treatment benefits.

About 70% of the participants in the experimental group successfully learned to self-regulate their NAcc using rtfMRI-based neurofeedback after only two training sessions. The learning group showed a higher BAS Drive score, higher tendency to select high-rewarding choices, and higher NAcc activation during the anticipation of monetary rewards compared with the nonlearning group. The learning group also showed higher baseline motivation than did the nonlearning group, suggesting the importance of motivation in predicting the effectiveness of rtfMRI-based neurofeedback training (Sokunbi, Linden, Habes, Johnston, & Ihssen, 2014).

If one is to translate rtfMRI-based neurofeedback training to clinical practice, a personalized intervention plan that maximizes its efficacy is crucial. Furthermore, the appropriate dosage of rtfMRI-based neurofeedback training requires further investigation (Sulzer, Haller, et al., 2013). It is interesting that some participants who successfully learned self-regulation in the first training session failed in the second session in our study. This suggests that one-session training may not be sufficient to achieve and maintain the training effect and that multiple sessions of training with appropriate intervals may be necessary to establish a stable training effect. A longer but optimal training time may contribute to the significant behavioral and brain changes after the rtfMRI neurofeedback.

The limited sample size of the *sham* control group means that the nonregulation results should be treated with caution. However, the specificity of rtfMRI training on the NAcc and the ventral striatum have been well established in the literature (Greer et al., 2014; Kirsch et al., 2016; MacInnes et al., 2016). It should also be noted that the sample size of both the experimental and *sham* control groups in this study was comparable to those in most other similar studies in the extant literature (Chiew, LaConte, & Graham, 2012; Ruiz, Buyukturkoglu, Rana, Birbaumer, & Sitaram, 2014). The other limitation was the potential gender bias in this study. Although there is no reported gender difference in real-time neurofeedback training, some evidence has suggested that gender difference on the pleasure experience, memory, and beliefs may be associated with NAcc activation (Kim-Prieto, Diener, Tamir, Scollon, & Diener, 2005; Robinson & Clore, 2002). Thus, to avoid the influence of gender difference, we included only female participants in this study. It is unclear whether rtfMRI neurofeedback is equally efficacious in male individuals. Finally, the present study examined only the short-term effect of self-regulation of NAcc through rtfMRI-based neurofeedback training. Future studies should examine the generalization effect by recruiting more ecologically valid measures to evaluate its effect over a longer period.

Conclusion

Activation of the NAcc could be volitionally regulated using rtfMRI-based neurofeedback training in healthy people. Baseline motivation may influence its effectiveness. People who were successful in learning self-regulation had higher baseline motivation than did those who did not acquire the skill. Real-time neurofeedback training on the NAcc may be able to improve behavioral manifestations of motivation and modify the reward circuit. This technique may have clinical potential for alleviating amotivation and anhedonia in patients with schizophrenia and other related disorders.

References

Beck, A., Schlagenhauf, F., Wüstenberg, T., Hein, J., Kienast, T., Kahnt, T., . . . Wrase, J. (2009). Ventral striatal activation during reward anticipation correlates with impulsivity in alcoholics. *Biological Psychiatry, 66,* 734–742. http://dx.doi.org/10.1016/j.biopsych.2009.04.035

Berridge, K. C. (2003). Pleasures of the brain. *Brain and Cognition, 52,* 106–128. http://dx.doi.org/10.1016/S0278-2626(03)00014-9

Berridge, K. C. (2007). The debate over dopamine's role in reward: The case for incentive salience. *Psychopharmacology, 191,* 391–431. http://dx.doi.org/10.1007/s00213-006-0578-x

Berridge, K. C., & Robinson, T. E. (1998). What is the role of dopamine in reward: Hedonic impact, reward learning, or incentive salience? *Brain Research Reviews, 28,* 309–369. http://dx.doi.org/10.1016/S0165-0173(98)00019-8

Carver, C. S., & White, T. L. (1994). Behavioral inhibition, behavioral activation, and affective responses to impending reward and punishment: The BIS/BAS Scales. *Journal of Personality and Social Psychology, 67,* 319–333. http://dx.doi.org/10.1037/0022-3514.67.2.319

Cauda, F., Cavanna, A. E., D'agata, F., Sacco, K., Duca, S., & Geminiani, G. C. (2011). Functional connectivity and coactivation of the nucleus accumbens: A combined functional connectivity and structure-based meta-analysis. *Journal of Cognitive Neuroscience, 23,* 2864–2877. http://dx.doi.org/10.1162/jocn.2011.21624

Chan, R. C. K., Li, Z., Li, K., Zeng, Y.-w., Xie, W.-z., Yan, C., . . . Jin, Z. (2016). Distinct processing of social and monetary rewards in late adolescents with trait anhedonia. *Neuropsychology, 30,* 274–280. http://dx.doi.org/10.1037/neu0000233

Chan, R. C. K., Shi, Y.-f., Lai, M.-k., Wang, Y.-n., Wang, Y., & Kring, A. M. (2012). The Temporal Experience of Pleasure Scale (TEPS): Exploration and confirmation of factor structure in a healthy Chinese sample. *PLoS ONE, 7*(4), e35352. http://dx.doi.org/10.1371/journal.pone.0035352

Chiew, M., LaConte, S. M., & Graham, S. J. (2012). Investigation of fMRI neurofeedback of differential primary motor cortex activity using kinesthetic motor imagery. *NeuroImage, 61,* 21–31. http://dx.doi.org/10.1016/j.neuroimage.2012.02.053

Cordes, J. S., Mathiak, K. A., Dyck, M., Alawi, E. M., Gaber, T. J., Zepf, F. D., . . . Mathiak, K. (2015). Cognitive and neural strategies during control of the anterior cingulate cortex by fMRI neurofeedback in patients with schizophrenia. *Frontiers in Behavioral Neuroscience, 9,* 169. http://dx.doi.org/10.3389/fnbeh.2015.00169

Cox, R. W. (1996). AFNI: software for analysis and visualization of functional magnetic resonance neuroimages. *Computers and Biomedical Research, 29,* 162–173.

deCharms, R. C. (2008). Applications of real-time fMRI. *Nature Reviews Neuroscience, 9,* 720–729. http://dx.doi.org/10.1038/nrn2414

Favrod, J., Giuliani, F., Ernst, F., & Bonsack, C. (2010). Anticipatory pleasure skills training: A new intervention to reduce anhedonia in schizophrenia. *Perspectives in Psychiatric Care, 46,* 171–181. http://dx.doi.org/10.1111/j.1744-6163.2010.00255.x

Ferenczi, E. A., Zalocusky, K. A., Liston, C., Grosenick, L., Warden, M. R., Amatya, D., . . . Deisseroth, K. (2016, January 1). Prefrontal cortical regulation of brainwide circuit dynamics and reward-related behavior. *Science, 351*(6268), aac9698. http://dx.doi.org/10.1126/science.aac9698

Friston, K. J. (2007). *Statistical parametric mapping: the analysis of funtional brain images* (1st ed.). Amsterdam, Boston: Elsevier/Academic Press.

Fornito, A., Harrison, B. J., Goodby, E., Dean, A., Ooi, C., Nathan, P. J., . . . Bullmore, E. T. (2013). Functional dysconnectivity of corticostriatal circuitry as a risk phenotype for psychosis. *Journal of the American Medical Association Psychiatry, 70,* 1143–1151. http://dx.doi.org/10.1001/jamapsychiatry.2013.1976

Friston, K. J., Williams, S., Howard, R., Frackowiak, R. S., & Turner, R. (1996). Movement-related effects in fMRI time-series. *Magnetic Resonance in Medicine, 35,* 346–355. http://dx.doi.org/10.1002/mrm.1910350312

Gard, D. E., Gard, M. G., Kring, A. M., & John, O. P. (2006). Anticipatory and consummatory components of the experience of pleasure: A scale development study. *Journal of Research in Personality, 40,* 1086–1102. http://dx.doi.org/10.1016/j.jrp.2005.11.001

Gong, Y. X. (1992). *Manual of Wechsler Adult Intelligence Scale-Chinese Version*. Changsha, China: Chinese Map Press.

Greer, S. M., Trujillo, A. J., Glover, G. H., & Knutson, B. (2014). Control of nucleus accumbens activity with neurofeedback. *NeuroImage, 96,* 237–244. http://dx.doi.org/10.1016/j.neuroimage.2014.03.073

Haber, S. N., & Knutson, B. (2010). The reward circuit: Linking primate anatomy and human imaging. *Neuropsychopharmacology, 35,* 4–26. http://dx.doi.org/10.1038/npp.2009.129

Heerey, E. A., & Gold, J. M. (2007). Patients with schizophrenia demonstrate dissociation between affective experience and motivated behavior. *Journal of Abnormal Psychology, 116,* 268–278. http://dx.doi.org/10.1037/0021-843X.116.2.268

Huang, J., Yang, X.-h., Lan, Y., Zhu, C.-y., Liu, X.-q., Wang, Y. F., . . . Chan, R. C. (2016). Neural substrates of the impaired effort expenditure decision making in schizophrenia. *Neuropsychology, 30,* 685–696. http://dx.doi.org/10.1037/neu0000284

Jenkinson, M., Beckmann, C. F., Behrens, T. E., Woolrich, M. W., & Smith, S. M. (2012). Fsl. *Neuroimage, 62,* 782–790. http://dx.doi.org/10.1016/j.neuroimage.2011.09.015

Juckel, G., Schlagenhauf, F., Koslowski, M., Filonov, D., Wüstenberg, T., Villringer, A., . . . Heinz, A. (2006). Dysfunction of ventral striatal reward prediction in schizophrenic patients treated with typical, not atypical, neuroleptics. *Psychopharmacology, 187,* 222–228. http://dx.doi.org/10.1007/s00213-006-0405-4

Juckel, G., Schlagenhauf, F., Koslowski, M., Wüstenberg, T., Villringer, A., Knutson, B., . . . Heinz, A. (2006). Dysfunction of ventral striatal reward prediction in schizophrenia. *NeuroImage, 29,* 409–416. http://dx.doi.org/10.1016/j.neuroimage.2005.07.051

Kim-Prieto, C., Diener, E., Tamir, M., Scollon, C., & Diener, M. (2005). Integrating the diverse definitions of happiness: A time-sequential framework of subjective well-being. *Journal of Happiness Studies, 6,* 261–300. http://dx.doi.org/10.1007/s10902-005-7226-8

Kirsch, M., Gruber, I., Ruf, M., Kiefer, F., & Kirsch, P. (2016). Real-time functional magnetic resonance imaging neurofeedback can reduce striatal cue-reactivity to alcohol stimuli. *Addiction Biology, 21,* 982–992. http://dx.doi.org/10.1111/adb.12278

Knutson, B., Bhanji, J. P., Cooney, R. E., Atlas, L. Y., & Gotlib, I. H. (2008). Neural responses to monetary incentives in major depression. *Biological Psychiatry, 63,* 686–692. http://dx.doi.org/10.1016/j.biopsych.2007.07.023

Knutson, B., Fong, G. W., Adams, C. M., Varner, J. L., & Hommer, D. (2001). Dissociation of reward anticipation and outcome with event-related fMRI. *NeuroReport, 12,* 3683–3687. http://dx.doi.org/10.1097/00001756-200112040-00016

Knutson, B., & Gibbs, S. E. B. (2007). Linking nucleus accumbens dopamine and blood oxygenation. *Psychopharmacology, 191,* 813–822. http://dx.doi.org/10.1007/s00213-006-0686-7

Knutson, B., Westdorp, A., Kaiser, E., & Hommer, D. (2000). FMRI visualization of brain activity during a monetary incentive delay task. *NeuroImage, 12,* 20–27. http://dx.doi.org/10.1006/nimg.2000.0593

Kring, A. M., & Barch, D. M. (2014). The motivation and pleasure dimension of negative symptoms: Neural substrates and behavioral outputs. *European Neuropsychopharmacology, 24,* 725–736. http://dx.doi.org/10.1016/j.euroneuro.2013.06.007

Kringelbach, M. L., & Berridge, K. C. (2009). Towards a functional neuroanatomy of pleasure and happiness. *Trends in Cognitive Sciences, 13,* 479–487. http://dx.doi.org/10.1016/j.tics.2009.08.006

Lawrence, E. J., Su, L., Barker, G. J., Medford, N., Dalton, J., Williams, S. C. R., . . . David, A. S. (2014). Self-regulation of the anterior insula: Reinforcement learning using real-time fMRI neurofeedback. *NeuroImage, 88,* 113–124. http://dx.doi.org/10.1016/j.neuroimage.2013.10.069

Li, Y. Z., Zhang, Y., Jiang, Y., Li, H., Mi, S., Yi, G. J., . . . Jiang, Y. (2008). The Chinese version of the BIS/BAS Scale: Reliability and validity. *Chinese Mental Health Journal, 22,* 613–616.

Lui, S. S. Y., Liu, A. C. Y., Chui, W. W. H., Li, Z., Geng, F., Wang, Y., . . . Chan, R. C. K. (2016). The nature of anhedonia and avolition in patients with first-episode schizophrenia. *Psychological Medicine, 46,* 437–447. http://dx.doi.org/10.1017/S0033291715001968

MacInnes, J. J., Dickerson, K. C., Chen, N.-k., & Adcock, R. A. (2016). Cognitive neurostimulation: Learning to volitionally sustain ventral tegmental area activation. *Neuron, 89,* 1331–1342. http://dx.doi.org/10.1016/j.neuron.2016.02.002

Mathiak, K. A., Alawi, E. M., Koush, Y., Dyck, M., Cordes, J. S., Gaber, T. J., . . . Mathiak, K. (2015). Social reward improves the voluntary control over localized brain activity in fMRI-based neurofeedback training. *Frontiers in Behavioral Neuroscience, 9,* 136. http://dx.doi.org/10.3389/fnbeh.2015.00136

Murphy, K., Birn, R. M., Handwerker, D. A., Jones, T. B., & Bandettini, P. A. (2009). The impact of global signal regression on resting state correlations: Are anti-correlated networks introduced? *NeuroImage, 44,* 893–905. http://dx.doi.org/10.1016/j.neuroimage.2008.09.036

Nguyen, A., Frobert, L., McCluskey, I., Golay, P., Bonsack, C., & Favrod, J. (2016). Development of the Positive Emotions Program for Schizophrenia: An intervention to improve pleasure and motivation in schizophrenia. *Frontiers in Psychiatry, 7,* 13. http://dx.doi.org/10.3389/fpsyt.2016.00013

Paret, C., Kluetsch, R., Ruf, M., Demirakca, T., Hoesterey, S., Ende, G., & Schmahl, C. (2014). Down-regulation of amygdala activation with real-time fMRI neurofeedback in a healthy female sample. *Frontiers in Behavioral Neuroscience, 8,* 299. http://dx.doi.org/10.3389/fnbeh.2014.00299

Pizzagalli, D. A. (2014). Depression, stress, and anhedonia: Toward a synthesis and integrated model. *Annual Review of Clinical Psychology, 10,* 393–423. http://dx.doi.org/10.1146/annurev-clinpsy-050212-185606

Pizzagalli, D. A., Holmes, A. J., Dillon, D. G., Goetz, E. L., Birk, J. L., Bogdan, R., . . . Fava, M. (2009). Reduced caudate and nucleus accumbens response to rewards in unmedicated individuals with major depressive disorder. *American Journal of Psychiatry, 166,* 702–710. http://dx.doi.org/10.1176/appi.ajp.2008.08081201

Radua, J., Schmidt, A., Borgwardt, S., Heinz, A., Schlagenhauf, F., McGuire, P., & Fusar-Poli, P. (2015). Ventral striatal activation during reward processing in psychosis: A neurofunctional meta-analysis. *Journal of the American Medical Association Psychiatry, 72,* 1243–1251. http://dx.doi.org/10.1001/jamapsychiatry.2015.2196

Robinson, M. D., & Clore, G. L. (2002). Belief and feeling: Evidence for an accessibility model of emotional self-report. *Psychological Bulletin, 128,* 934–960. http://dx.doi.org/10.1037/0033-2909.128.6.934

Ruiz, S., Buyukturkoglu, K., Rana, M., Birbaumer, N., & Sitaram, R. (2014). Real-time fMRI brain computer interfaces: Self-regulation of single brain regions to networks. *Biological Psychology, 95,* 4–20. http://dx.doi.org/10.1016/j.biopsycho.2013.04.010

Saad, Z. S., Gotts, S. J., Murphy, K., Chen, G., Jo, H. J., Martin, A., & Cox, R. W. (2012). Trouble at rest: How correlation patterns and group differences become distorted after global signal regression. *Brain Connectivity, 2,* 25–32. http://dx.doi.org/10.1089/brain.2012.0080

Salamone, J. D., Correa, M., Farrar, A. M., Nunes, E. J., & Pardo, M. (2009). Dopamine, behavioral economics, and effort. *Frontiers in Behavioral Neuroscience, 3,* 13. http://dx.doi.org/10.3389/neuro.08.013.2009

Schlaepfer, T. E., Cohen, M. X., Frick, C., Kosel, M., Brodesser, D., Axmacher, N., . . . Sturm, V. (2008). Deep brain stimulation to reward circuitry alleviates anhedonia in refractory major depression. *Neuropsychopharmacology, 33,* 368–377. http://dx.doi.org/10.1038/sj.npp.1301408

Schultz, W. (1998). Predictive reward signal of dopamine neurons. *Journal of Neurophysiology, 80,* 1–27. http://dx.doi.org/10.1152/jn.1998.80.1.1

Schultz, W., Dayan, P., & Montague, P. R. (1997, March 14). A neural substrate of prediction and reward. *Science, 275,* 1593–1599. http://dx.doi.org/10.1126/science.275.5306.1593

Sherwood, M. S., Kane, J. H., Weisend, M. P., & Parker, J. G. (2016). Enhanced control of dorsolateral prefrontal cortex neurophysiology with real-time functional magnetic resonance imaging (rt-fMRI) neurofeedback training and working memory practice. *NeuroImage, 124,* 214–223. http://dx.doi.org/10.1016/j.neuroimage.2015.08.074

Sitaram, R., Caria, A., Veit, R., Gaber, T., Ruiz, S., & Birbaumer, N. (2014). Volitional control of the anterior insula in criminal psychopaths using real-time fMRI neurofeedback: A pilot study. *Frontiers in Behavioral Neuroscience, 8,* 344. http://dx.doi.org/10.3389/fnbeh.2014.00344

Sokunbi, M. O., Linden, D. E. J., Habes, I., Johnston, S., & Ihssen, N. (2014). Real-time fMRI brain-computer interface: Development of a "motivational feedback" subsystem for the regulation of visual cue reactivity. *Frontiers in Behavioral Neuroscience, 8,* 392. http://dx.doi.org/10.3389/fnbeh.2014.00392

Sulzer, J., Haller, S., Scharnowski, F., Weiskopf, N., Birbaumer, N., Blefari, M. L., . . . Sitaram, R. (2013). Real-time fMRI neurofeedback: Progress and challenges. *NeuroImage, 76,* 386–399. http://dx.doi.org/10.1016/j.neuroimage.2013.03.033

Sulzer, J., Sitaram, R., Blefari, M. L., Kollias, S., Birbaumer, N., Stephan, K. E., . . . Gassert, R. (2013). Neurofeedback-mediated self-regulation of the dopaminergic midbrain. *NeuroImage, 83,* 817–825. http://dx.doi.org/10.1016/j.neuroimage.2013.05.115

Treadway, M. T., Buckholtz, J. W., Schwartzman, A. N., Lambert, W. E., & Zald, D. H. (2009). Worth the "EEfRT"? The effort expenditure for rewards task as an objective measure of motivation and anhedonia. *PLoS ONE, 4*(8), e6598. http://dx.doi.org/10.1371/journal.pone.0006598

Tzourio-Mazoyer, N., Landeau, B., Papathanassiou, D., Crivello, F., Etard, O., Delcroix, N., . . . Joliot, M. (2002). Automated anatomical labeling of activations in SPM using a macroscopic anatomical parcellation of the MNI MRI single-subject brain. *NeuroImage, 15,* 273–289. http://dx.doi.org/10.1006/nimg.2001.0978

Wacker, J., Dillon, D. G., & Pizzagalli, D. A. (2009). The role of the nucleus accumbens and rostral anterior cingulate cortex in anhedonia: Integration of resting EEG, fMRI, and volumetric techniques. *NeuroImage, 46,* 327–337. http://dx.doi.org/10.1016/j.neuroimage.2009.01.058

Wang, J., Wang, X., Xia, M., Liao, X., Evans, A., & He, Y. (2015). GRETNA: a graph theoretical network analysis toolbox for imaging connectomics. *Frontiers in Human Neuroscience, 9,* 386. http://dx.doi.org/10.3389/fnhum.2015.00386

Watts, D. J., & Strogatz, S. H. (1998). Collective dynamics of "small-world" networks. *Nature, 393,* 440–442. http://dx.doi.org/10.1038/30918

Wrase, J., Schlagenhauf, F., Kienast, T., Wüstenberg, T., Bermpohl, F., Kahnt, T., . . . Heinz, A. (2007). Dysfunction of reward processing correlates with alcohol craving in detoxified alcoholics. *NeuroImage, 35,* 787–794. http://dx.doi.org/10.1016/j.neuroimage.2006.11.043

Wyvell, C. L., & Berridge, K. C. (2000). Intra-accumbens amphetamine increases the conditioned incentive salience of sucrose reward: Enhancement of reward "wanting" without enhanced "liking" or response reinforcement. *Journal of Neuroscience, 20,* 8122–8130. http://dx.doi.org/10.1523/JNEUROSCI.20-21-08122.2000

Yan, C.-G., Craddock, R. C., He, Y., & Milham, M. P. (2013). Addressing head motion dependencies for small-world topologies in functional connectomics. *Frontiers in Human Neuroscience, 7,* 910. http://dx.doi.org/10.3389/fnhum.2013.00910

Yan, C. G., Wang, X. D., Zuo, X. N., & Zang, Y. F. (2016). DPABI: Data Processing & Analysis for (Resting-State) Brain Imaging. *Neuroinformatics, 14,* 339–351. http://dx.doi.org/10.1007/s12021-016-9299-4

Zhang, G., Yao, L., Zhang, H., Long, Z., & Zhao, X. (2013). Improved working memory performance through self-regulation of dorsal lateral prefrontal cortex activation using real-time fMRI. *PLoS ONE, 8*(8), e73735. http://dx.doi.org/10.1371/journal.pone.0073735

Zotev, V., Krueger, F., Phillips, R., Alvarez, R. P., Simmons, W. K., Bellgowan, P., . . . Bodurka, J. (2011). Self-Regulation of amygdala activation using real-time fMRI neurofeedback. *PLoS ONE, 6*(9), e24522. http://dx.doi.org/10.1371/journal.pone.0024522

Received March 18, 2017
Revision received September 11, 2017
Accepted September 11, 2017 ■